Measures of Unobservability

Arthur J. Krener and Kayo Ide

***Abstract*— An observed nonlinear dynamics is observable if the mapping from initial condition to output trajectory is one to one. The standard tool for checking observability is the observability rank condition but this only gives a yes or no answer. It does not measure how observable or unobservable the system is. Moreover it requires the ability to differentiate the dynamics and the observations. We introduce new tools, the local unobservability index and the local estimation condition number, to measure the degree of observability or unobservability of a system. To compute these one only needs the ability to simulate the system. We apply these tools to find the best location to put a sensor to observe the flow induced by two point vortices.**

I. INTRODUCTION

Consider an observed dynamical system.

$$\begin{aligned} \dot{x} &= f(x) \\ y &= h(x) \\ x(0) &= x^0 \end{aligned} \tag{1}$$

where x is n dimensional and y is p dimensional. The system is observable over the interval $[0, T]$ if the mapping from initial state x^0 to output trajectory $y(0:T)$ is one to one. The notation $y(0:T)$ means the mapping $t \mapsto y(t)$ for $0 \le t < T$. It is locally observable over the interval $[0, T]$ if this mapping is locally one to one. It is short time locally observable if it locally observable for all $T > 0$.

The usual tool for checking short time locally observability is the observability rank condition [2], [6], [7]. To define it we need some other concepts. The differential of a function h is

$$dh(x) = \frac{\partial h}{\partial x}(x)$$

If $x \in \mathbb{R}^n$ and $h(x) \in \mathbb{R}^p$ then $dh(x)$ is a $p \times n$ matrix valued function of x. The Lie derivative of h by f as

$$L_f(h)(x) = dh(x)f(x)$$

This is a $p \times 1$ valued function of x. This operation can be iterated

$$L_f^k(h)(x) = dL_f^{k-1}(h)(x)f(x)$$

The observed system (1) satisfies the observability rank condition at x if the $(k+1)p \times n$ matrix

$$\begin{bmatrix} dh(x) \\ \vdots \\ dL_f^k(h)(x) \end{bmatrix} \tag{2}$$

has rank n for some k.

The observability rank condition essentially determines whether the system is short time locally observable. If the system satisfies the observability rank condition at every $x \in \mathbb{R}^n$ then it is short time locally observable. If the system fails to satisfy the observability rank condition on an open subset of $\mathbb{R}^n$ then it is not short time locally observable [2].

But it does not tell us how easy is it to observe the system. Moreover even if the system is given analytically, it can be very difficult to compute. If the system is given numerically (by computer code) it can't be computed. We need other tools to measure degrees of observability and unobservability and one that can be applied to systems that are given numerically. To overcome these difficulties we return to an old tool, the local observability gramian and some related numbers.

As a first step in this direction consider the local linear approximating system around the the state trajectory $x^0(t)$ and output trajectory $y^0(t)$ starting at x^0,

$$\begin{aligned} \dot{\delta x} &= F(t)\delta x \\ \delta y &= H(t)\delta x \\ \delta x(0) &= \delta x^0 \end{aligned} \tag{3}$$

where

$$\begin{aligned} \delta x &\approx x - x^0(t) \\ \delta y &\approx y - y^0(t) \\ F(t) &= \frac{\partial f}{\partial x}(x^0(t)) \\ H(t) &= \frac{\partial h}{\partial x}(x^0(t)) \end{aligned}$$

The linear approximating system defines a linear mapping from small changes in the initial condition δx^0 to changes in the output $\delta y(0:T)$ that is tangent at x^0 to the corresponding nonlinear mapping from $x(0)$ to $y(0:T)$ defined by (1). The *local singular values* at x^0 of the nonlinear mapping defined by (1) are the singular values of its tangent linear mapping defined by (3). If the local singular values at x^0 are all large then it is relatively easy to invert the mapping from $x(0)$ to $y(0:T)$ near x^0. In other words it is relatively easy to distinguish initial states around x^0 from their output trajectories.

Consider any estimation scheme that is exact when there is no observation noise present, that is, the estimation scheme exactly inverts the map from $x(0)$ to $y(0:T)$ defined by the nonlinear system (1). If this estimation scheme is smooth then it has a local singular value at $y^0(0:T)$ that is at least as large as the reciprocal of the smallest local singular value of the nonlinear system (1) at x^0. Therefore the reciprocal of the smallest local singular value is a measure of how

This work was supported in part by by NSF DMS-0505677.

A. J. Krener is with the Department of Applied Mathematics, Naval Postgraduate School, Monterey, CA 93943, USA ajkrener@nps.edu

K. Ide is with the Department of Atmospheric and Oceanic Sciences, University of Maryland, College Park, MD 20742, USA ide@umd.edu

difficult it is estimate the initial condition from the output. If this reciprocal is very large then observation noise can have a large impact on the estimation error. We call the reciprocal of the smallest local singular value the *local unobervability index* of the nonlinear system (1).

Another measure of unobservability is the ratio of the largest local singular value to the smallest. We call this the *local estimation condition number* of the nonlinear system (1). If this is large then the effect on the output caused by a small change in the initial condition in one direction can swamp the effect on the output of a change in another direction. In other words the estimation problem is ill-conditioned near states with large local estimation condition number.

To compute the local singular values of the nonlinear system (1), we compute its local observabilty gramian $P(x^0)$. This is the observability gramian over $[0,T]$ of the linear approximating system (3). The square roots of eigenvalues of $P(x^0)$ are the local singular values of (1) at x^0. The local unobservability index is the reciprocal of the square root of the smallest eigenvalue of $P(x^0)$. The local estimation condition number is the square root of the ratio of the largest eigenvalue of $P(x^0)$ to its smallest.

Let $\Phi(t)$ be the fundamental matrix solution of the linear dynamics (3),

$$\begin{aligned}\frac{\mathrm{d}}{\mathrm{dt}}\Phi(t) &= F(t)\Phi(t)\\ \Phi(0) &= I\end{aligned}$$

then the local observability gramian is

$$P(x^0) = \int_0^T \Phi'(t)H'(t)H(t)\Phi(t)\mathrm{dt}$$

This can be expensive to compute as it requires computing F, H, Φ so we introduce the empirical local observability gramian. Given the length of a small displacement $\epsilon > 0$ of the state, let $x^{\pm i} = x^0 \pm \epsilon \mathbf{e}^i$ and $y^{\pm i}(t)$ be the corresponding output, $\mathbf{e}^i$ is the i^{th} unit vector in $I\!R^n$. The empirical local observability gramian at x^0 is the $n \times n$ matrix $P(x^0)$ whose (i,j) component is

$$\frac{1}{4\epsilon^2}\int_0^T (y^{+i}(t) - y^{-i}(t))'(y^{+j}(t) - y^{-j}(t))\ dt \tag{4}$$

This is much easier to compute because it requires only the ability to simulate the observed dynamical system. It can be shown that if the system is smooth then the empirical local observability gramian converges to the local observability gramian as $\epsilon \to 0$. To simplify terminology henceforth we shall refer to the empirical local observability gramian (4) as the *local observability gramian*.

Remarks:

- Moore [11] empirically calculated the observability gramian for a linear system around the zero state in a similar fashion.
- Lall, Marsden and Glavski [9] empirically calculated the observability gramian for a nonlinear system around an equilibrium state in a similar fashion.
- Before the computing the local observability gramian, the state coordinates x should be properly scaled otherwise the relative size of the eigenvalues may mean very little.
- The output coordinates y should also be scaled. If there is additive noise present in the observation, the output coordinates y should be chosen so that the noise covariance is the identity.
- If the standard size of each state coordinate is of order one then a reasonable choice of ϵ is order 0.01 or 0.001. In the example below we used both and it did not make much difference.
- The local observability gramian (and its eigenvalues) is a nondecreasing function of the interval $[0,T]$. Hence the local unobservability index is nonincreasing function of T. However the local estimation condition number need not be a monotone function of T.
- Suppose the observation is partitioned into two subvectors $y_1$and y_2 . Then the total local observability gramian $P(x^0)$ is a sum of the separate local observability gramians, $P_1(x^0)$ and $P_2(x^0)$. As $P_2(x^0)$ is added to $P_1(x^0)$, the changes in the local unobservability index and the local estimation condition number measure how much additional observability y_2 adds to y_1. The local unobservability index will not increase but the local estimation condition number might.
- One need not compute the full local observability gramian, one can restrict to changes of the initial state in the most important state directions to measure their observability.
- The local observability gramian can be expanded to measure the effect of parameter changes on the output. For nonlinear systems the distinction between parameters and states is rather moot as parameters can always be viewed as additional states with time derivative zero.
- There are methods to measure the sensitivity of an estimation scheme to an observation, e.g. [10], but these depend heavily on the estimation method that is being used. The local unobservability index and the local estimation condition measure how difficult it is to accurately estimate the initial state from the output by any and all schemes. Moreover they do not require an adjoint system to compute them.

To illustrate the usefulness of the local unobservability index and the local estimation condition number, we apply them in the following sections to finding the best locations for an observation to determine the centers and strengths of two vortex flow. The observability rank condition was used to determine the observability of such flows in [6] and [7]. Other work on the controllability and observability of point vortex systems can be found in [3], [4], [5], [12] and [13] [14].

II. Two Vortex Flow

For an introduction to vortex flow we refer the reader to [1]. The configuration of two point vortices in the plane is completely determined by six state variables

$$x = (x_{11}, x_{12}, x_{13}, x_{21}, x_{22}, x_{23})'$$

where x_{i1}, x_{i2} is the center of the i^{th} vortex and $2\pi x_{i3}$ is its circulation . The flow velocity at a point (ξ_1, ξ_2) in the flow domain induced by the i^{th} vortex is

$$\mathbf{u}_i(\xi, x) = \frac{x_{i3}}{r_1^2} \begin{bmatrix} x_{i2} - \xi_2 \\ \xi_1 - x_{i1} \end{bmatrix} \tag{5}$$

where

$$r_i^2 = (\xi_1 - x_{i1})^2 + (\xi_2 - x_{i2})^2.$$

The total flow is the sum of the individual vortex flows,

$$\mathbf{u}(\xi, x) = \mathbf{u}_1(\xi, x) + \mathbf{u}_2(\xi, x) \tag{6}$$

This flow is inviscid, incompressible and irrotational and except for its singularities at the centers of the vortices it is an exact solution of the two dimensional Euler equations. It has a stream function

$$\psi(\xi, x) = -x_{13} \ln |\xi - (x_{11}, x_{12})'| - x_{23} \ln |\xi - (x_{21}, x_{22})'|$$

Each vortex moves under the influence of the other vortex and their circulations don't change so the dynamics is

$$\begin{bmatrix} \dot{x}_{11} \\ \dot{x}_{12} \\ \dot{x}_{13} \\ \dot{x}_{21} \\ \dot{x}_{22} \\ \dot{x}_{23} \end{bmatrix} = \frac{1}{r^2} \begin{bmatrix} x_{23}(x_{22} - x_{12}) \\ x_{23}(x_{11} - x_{21}) \\ 0 \\ x_{13}(x_{12} - x_{22}) \\ x_{13}(x_{21} - x_{11}) \\ 0 \end{bmatrix} \tag{7}$$

where r is the constant

$$r^2 = (x_{11} - x_{21})^2 + (x_{12} - x_{22})^2.$$

But vortex flow is an idealization because of the singularities at the centers of the vorticies, all of the vorticity is concentrated there. So frequently a modified model, the Rankine vortex, is used instead [1], [4]. A Rankine vortex of radius R centered at x_{i1}, x_{i2} with circulation $2\pi x_{i3}$ induces the flow

$$\mathbf{u}_i^R(\xi, x) = \begin{cases} \dfrac{x_{i3}}{r_i^2} \begin{bmatrix} x_{i2} - \xi_2 \\ \xi_1 - x_{i1} \end{bmatrix} & \text{if} \quad r_i > R \\ \dfrac{x_{i3}}{R^2} \begin{bmatrix} x_{i2} - \xi_2 \\ \xi_1 - x_{i1} \end{bmatrix} & \text{if} \quad r_i \leq R \end{cases}$$

In this model the vorticity is constant inside a circle of radius R around the center of the vortex and zero elsewhere. The flow induced by two Rankine vortices is just their sum,

$$\mathbf{u}^R(\xi, x) = \mathbf{u}_1^R(\xi, x) + \mathbf{u}_2^R(\xi, x)$$

If the constant distance r between the centers exceeds R, the motion of the Rankine vortices is the same as before (7). We assume $r \geq R$ so that effect of vortex deformation can be neglected in vortex interaction.

III. Eulerian and Lagrangian Observations

An Eulerian observation is the fluid velocity at a fixed location ξ^0 in the flow

$$y = h(x) = \mathbf{u}(\xi^0, x) \tag{8}$$

A Lagrangian observation is the position or velocity of a particle $\xi(t)$ moving with the flow. We shall take it to be the velocity of the moving particle to make it comparable to an Eulerian observation. To model this as an observed dynamical system we follow [5], [8] and add the location of the observation as two extra states $\xi(t)$ of the dynamics,

$$\dot{\xi} = \mathbf{u}(\xi, x) \tag{9}$$

The new state is eight dimensional and its dynamics is given by (7) and (9). The Lagrangian observation is formally similar to the Euclidean observation (8)

$$y = h(x, \xi) = \mathbf{u}(\xi(t), x) \tag{10}$$

But the flow has singularities at centers of the vortices and this leads to numerical problems in computing the local observability gramian when an observation location is close to a vortex center. Hence we assume that we are observing Rankine vortices

$$y = h^R(x, \xi) = \mathbf{u}^R(\xi, x) \tag{11}$$

and the Lagrangian observation location obeys Rankine dynamics

$$\dot{\xi} = \mathbf{u}^R(\xi, x)$$

IV. Two Equal Vortices

Consider the flow induced by two equal vortices starting at $(1, 0)$ and $(-1, 0)$ both with circulation 2π. The two vortices rotate counterclockwise around the circle of radius 1 at opposite ends of a rotating diagonal. The period of rotation is 4π. The observations are assumed to be Rankine with $R = 0.2$ which is one tenth of the distance between the vortices.

Figure 1 shows the streamlines of the flow in a frame corotating with the centers of the vortices. Figure 2 shows the velocity field of the flow in the corotating frame. The origin is the center of rotation and is also a stagnation point of the flow. Notice that there are three saddle points at $(0, 0)$ and near $(\pm 2, 0)$ that corotate with the centers of the two vortices. There are also two corotating centers near $(0, \pm 2)$.

It was found in [6], [7] that the observability rank condition is satisfied unless the observation is made at $(0, 0)$. This is true for both an Eulerian or Lagrangian observation because the fluid velocity is zero at $(0, 0)$ so the two types of observations there are identical.

First we compute local unobservability index and the local estimation condition number over a full period of rotation $T = 4\pi$ of the vortices as a function of the (starting) location of an Eulerian (Lagrangian) observation.

Since it is computed over a full period the local observability gramian is rotationally symmetric with respect to the location of an Eulerian observation. Figure 3 shows the local unobservability index as a function of the radius $\pm|\xi|$ of a Eulerian observation made at ξ. Notice the log10 scale. The minimum, $10^{-0.55}$, occurs at $|\xi| = 1$ so the centers of the vortices pass through the location of the observation. The maximum, $10^{6.85}$, occurs at $\xi = (0, 0)$. The range of unobservability as measured by this index is over 7 orders of magnitude!

Figure 4 shows the local estimation condition number as a function of the location of a Eulerian observation. It confirms that the best place to make an Eulerian observation is on the circle of radius one where the local estimation condition number is $10^{1.75}$ and the worst place is at the origin where the local estimation condition number is $10^{7.9}$. Notice that the minimum local estimation condition number, $10^{1.5}$, which occurs at radius 1.36, is still large and therefore some states are always more observable than others regardless of the sensor location. The estimation problem is mildly ill-posed.

The dynamics (7), (9) is eight dimensional when we include as state variables the location ξ of the Lagrangian observer but presumably these extra states are known exactly. Hence we compute the partial local observability gramian with respect to changes in the original six states x. It is not a rotationally symmetric function of the starting location of a Lagrangian observation over a full period of rotation of the vortices.. Figure 5 shows the local unobservability index as a function of the starting location of the observation and Figure 6 shows the corresponding local estimation condition number. The spacing between the contour lines is 0.25 on the log10 scale. Hence a change of four contours indicates a change by factor of 10. What is not so evident in these contour plots is that there is a sharp peak at the origin and lesser peaks at the centers of the two vortices. The corresponding plots for an Eulerian observation had similar peaks at the origin but had local minima at the centers of the vortices. Presumably this is true because if an Eulerian observation starts at a vortex center it does not stay there as the center moves away. A Lagrangian observation that starts near a vortex center tends to rotate with the center.

Notice the obvious similarities between Figure 5 with the corotating streamlines, Figure 1. From Figure 5 we conclude that there are several places where one does not want to start a Lagrangian observation, near the origin, near the vortices and near the corotating centers. The best places to start a Lagrangian observation are in the "mask" around the vortices, close but not too close to the vortices.

Next we compute the local observability gramian over a twelfth of a period of rotation $T = \pi/3$. The gramian is no longer rotationally symmetric with respect to the location of an Eulerian observation. The local unobservability index is shown in Figure 6 and the local estimation condition number Figure 7. The best place to make an Eulerian observation seems to be at or near the vortices.

Poor places to make the observation are near the origin and along the line through the origin at $\pi/6$ angle to the ξ_1 axis. We believe the reason for the latter is the following. When $k = 2$ the matrix (2) is 6×6 so that this is the smallest k such that the observability rank condition could hold. Generally this matrix is of full rank except when the observation is made on the line between the vortices. In fact the determinant of this matrix changes sign as the observation location is moved through the line between the vortices. When the Eulerian observation is made on the line at $\pi/6$ angle to the ξ_1 axis, then for half of the observation period, $T = \pi/3$, this determinant is positive and half the time it is negative so the observation is as close to this line as is possible throughout the interval of observation. Apparently this causes a loss of observability.

Figures 9 and 10 show the local unobservability index and the local estimation condition number as a function of the starting location of a Lagrangian observation over a twelfth of a period of rotation, $T = \pi/3$.. Again the best place to start a Lagrangian observation is near but not too near the vortices. Poor places to start a Lagrangian observation are at the origin, close to the vortex centers, in the "smoke ring" surrounding the two vortices and along two rays at $\pi/6$ angle to the ξ_1 axis emanating from the corotating saddles near $(\pm 2, 0)$ in Figure 1. As can be seen from Figure 2 the "smoke ring" is almost corotating with vortices and it includes the corotating centers at $(0, \pm 2)$ of Figure 1. We believe the reason that the two rays are poor locations are that Lagrangian observations made there are as close as possible to the line through the centers of the vortices throughout the interval of observation.

The following tables give the minima for the various cases. First we consider the local unobservability index.

Unobservability Index	Eulerian	Lagrangian
Full Period	$10^{-0.55}$	$10^{-1.4}$
Partial Period	$10^{0.6}$	$10^{0.15}$

Next we consider the local estimation condition number.

Condition number	Eulerian	Lagrangian
Full Period	$10^{1.75}$	$10^{1.2}$
Partial Period	$10^{2.0}$	$10^{1.5}$

These tables confirm the superiority of the best Lagrangian observations over the best Eulerian observations. Notice also how significantly the local unobservability index decreases when we go from a partial to full period of observation. The local estimation condition number also decreases but not as dramatically. In fact it is over fifteen in all cases so the estimation problem is always mildly ill-posed.

The situation is much improved if a second observation is available. For instance the minimum of the local unobservability index is less than 10^{-3} for two Eulerian observations over a full period while the minimum of the local estimation condition number is less than $10^{0.7}$.

V. Conclusion

We have introduced two new tools, the local unobservability index and the local estimation condition number, for measuring the local observability of a nonlinear system and the well-posedness of the estimation problem. These tools allowed comparison of different observation schemes.

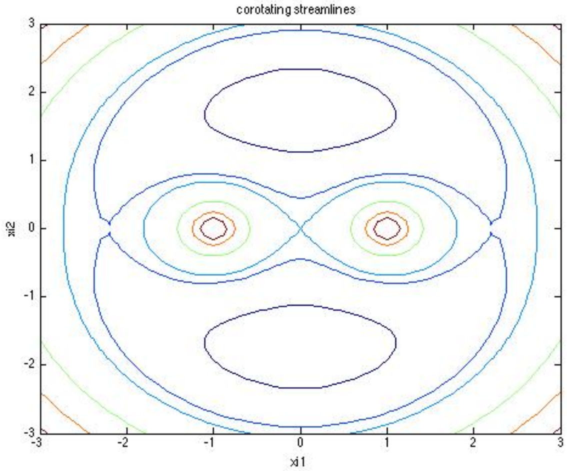

Fig. 1. Corotating steamlines

We applied these tools to finding the best locations for an Eulerian or Lagrangian observation of two vortex flow. The best Lagrangian locations are superior to the best Eulerian locations.

REFERENCES

[1] D. J. Acheson, *Elementary Fluid Dynamics,* Clarendon Press, Oxford, 1990.

[2] R. Hermann and A. J. Krener, Nonlinear Controllability and Observability, *IEEE Trans. Auto. Control*, vol. 22, 1977, pp. 728–740, 1977.

[3] K. Ide. and M. Ghil, Extended Kalman Filtering for Vortex Systems. Part I: Methodology and Point Vortices, *Dynamics of Atmospheres and Oceans*, vol. 27, 1997 , pp. 301–332.

[4] K. Ide. and M. Ghil, Extended Kalman Filtering for Vortex Systems. Part II: Rankine Vortices, *Dynamics of Atmospheres and Oceans*, vol. 27, 1997, pp. 333–350.

[5] K. Ide, L. Kuznetsov and C.K.R.T. Jones, Lagrangian Data Assimilation for Point Vortex Systems, *J. Turbulence* vol. 3, http://www.tandf.co.uk/journals/titles/14685248.asp, 2002.

[6] A. J. Krener, Observability of Vortex Flows, *in Fourty Seventh Conference on Decision and Control*, Cancun, Mexico, 2008. .

[7] A. J. Krener, Eulerian and Lagrangian Observability of Point Vortex Flows, *Tellus A* vol. xx, 2008, pp. xx-xx.

[8] L. Kuznetsov, K. Ide, and C.K.R.T. Jones, A Method for Assimilation of Lagrangian Data, *Monthly Weather Review*, vol. 131, 2003, pp. 2247–2260.

[9] S. Lall, J. E. Marsden and S. Glavski, A subspace approach to balanced truncation for model reduction of nonlinear control systems, *Int. J. Robust Nonlinear Control*, vol. 12, 2002, pp. 519-535.

[10] R. Langland and N. Baker, Estimation of observtion impact using the NRL atmospheric variational data assimilation adjoint system, *Tellus*, vol. 56A, pp. 289-202.

[11] B. C. Moore, Principle Component Analysis in Linear Systems: Controllability, Observability and Model Reduction, *IEEE Trans. Auto. Con.*, vol. 26, 1981 , pp. 17-32.

[12] G. Tadmor, Observers and Feedback Control for a Rotating Vortex Pair, *IEEE Transactions on Control Systems Technology*, vol 12, 2004, pp. 36–51.

[13] G. Tadmor and A. Banaszuk, Observer-based Control of Vortex Motion in a Combustor Recirculation Region, *IEEE Transactions on Control Systems Technology*, vol. 10, 2002, pp. 749–755.

[14] D. Vainchtein and I. Mezic, Control of a Vortex Pair Using a Weak External Flow, *J. Turbulence* vol. 3, 051 http://www.tandf.co.uk/journals/titles/14685248.asp, 2002.

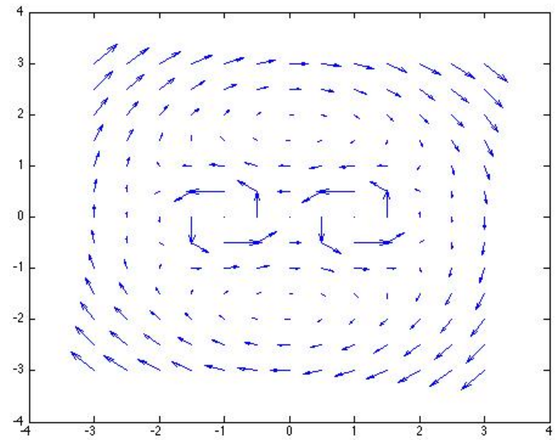

Fig. 2. Corotating flow field

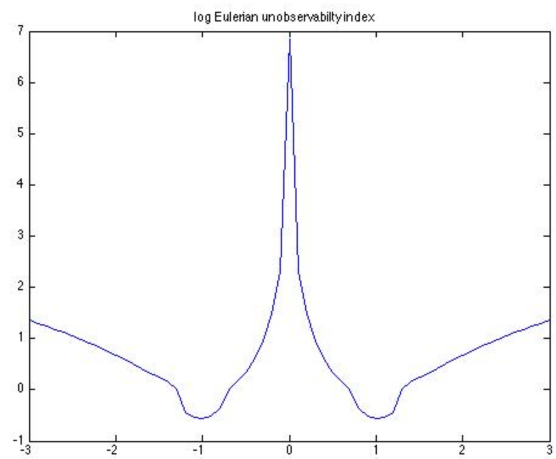

Fig. 3. Log of Eulerian unobservability index, full period

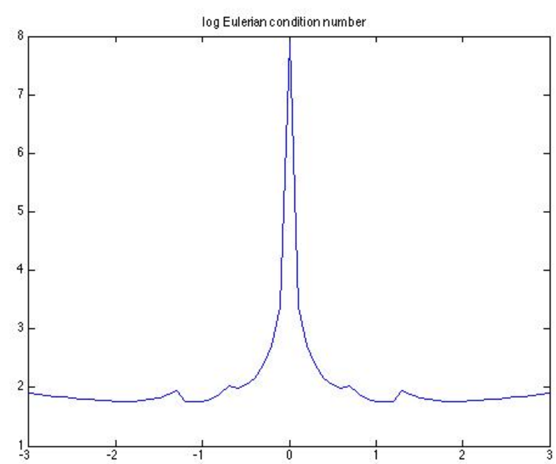

Fig. 4. Log of Eulerian estimation condition number, full period

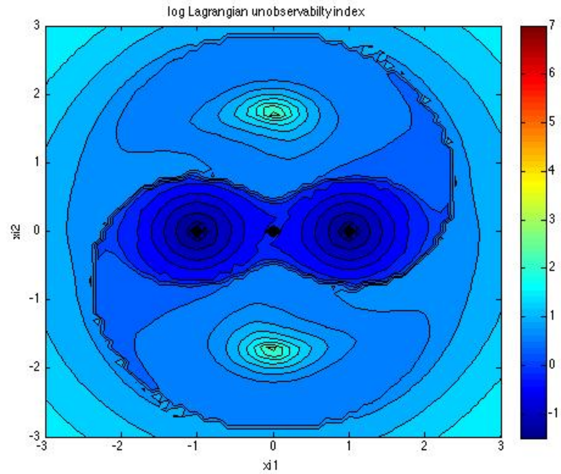

Fig. 5. Log of Lagrangrian unobservability index, full period

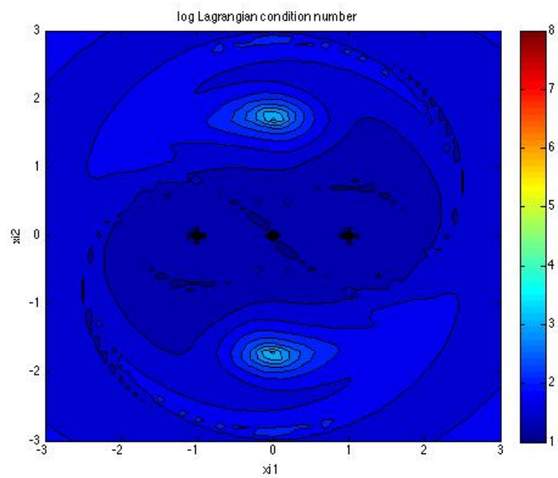

Fig. 6. Log of Lagrangian estimation condition number, full period

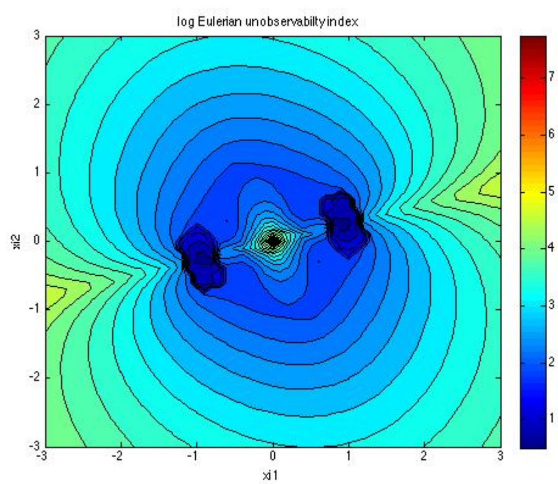

Fig. 7. Log of Eulerian unobservability index,, partial period

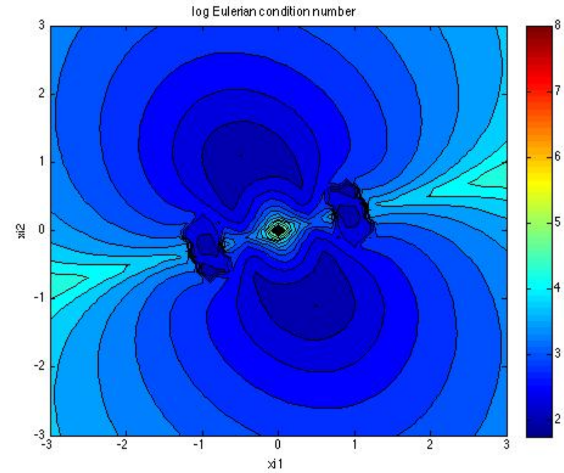

Fig. 8. Log of Eulerian estimation condition number, partial period

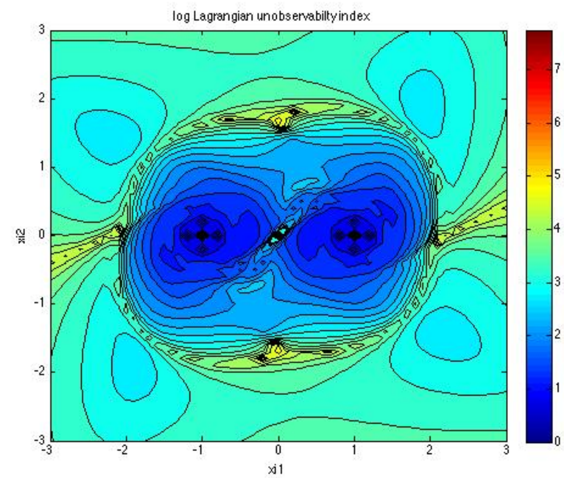

Fig. 9. Log of Lagrangian unobservability index, partial period

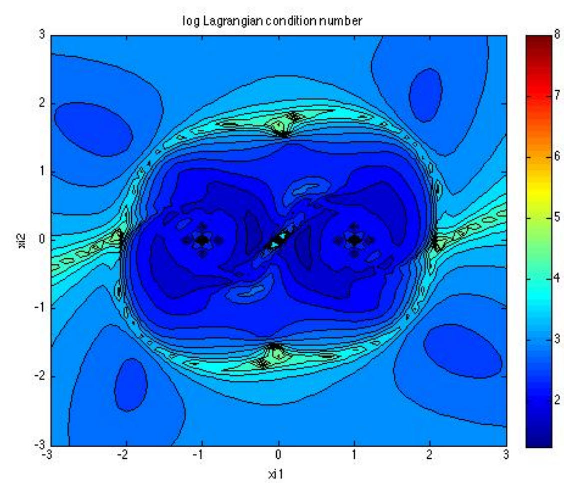

Fig. 10. Log of Lagrangian estimation condition number, partial period